

# Denuding the Boron Atom of B–H Interactions in Transition Metal–Boron Clusters

Catherine E. Housecroft

Institut für Anorganische Chemie, Universität Basel, Spitalstrasse 51, CH-4056 Basel, Switzerland

## 1 Introduction

The versatility of the bonding capabilities of boron is widely recognized, in particular with respect to the elemental state and in the chemistry of the boron hydrides (boranes).<sup>1–3</sup> Within discrete molecular chemistry, the icosahedral unit (1) is present in  $[B_{12}H_{12}]^{2-}$  and  $[C_2B_{10}H_{12}]$  as well as a range of heteroatomic clusters, the heteroatom(s) being from either the *p*- or *d*-blocks. In a closed icosahedral cluster, the boron atom is 6-coordinate–5-coordinate within the cage with an additional terminal B–X unit (X is usually H) pointing outside from the cage. If we consider that boron has only three valence electrons ( $[He]2s^22p^1$ ), then the connectivity number of six indicates that bonding within these icosahedral species is delocalized. The seminal works of Wade,<sup>4</sup> Williams,<sup>5</sup> and Mingos<sup>6</sup> have provided the basis for the now well-known Polyhedral Skeletal Electron Pair Theory (PSEPT) and the relationships between open- and closed-cage borane cluster compounds are clearly established. The structures of most single-cage boranes are based upon the series of deltahedra ( $\Delta$ -faced polyhedra) with between 5 and 12 vertices.

The replacement of BH units in a borane cluster by transition metal fragments, for example  $\{Fe(CO)_3\}$ ,  $\{\eta^5\text{-CpCo}\}$ , or  $\{\eta^6\text{-C}_6H_6\text{Ru}\}$ , can lead to metallaboranes which are structurally



(1)

Dr. Catherine E. Housecroft gained her B.Sc. in chemistry in 1976 and her Ph.D. in 1979 under the supervision of Professor Ken Wade, both from the University of Durham. After postdoctoral work at the University of Notre Dame, Indiana with Professor Tom Fehlner, Catherine was appointed as an Assistant Professor at the University of New Hampshire. In 1986, she moved to the University Chemical Laboratory in Cambridge (as a College Lecturer with Newnham and Trinity Colleges) and was appointed as a 1983 Royal Society Research Fellow in 1987, becoming, in 1990, a University Lecturer in Inorganic Chemistry at Cambridge.

In 1994 she moved to the Institut für Anorganische Chemie, Universität Basel where she currently holds a position of Privat Dozentin. Research interests have centred on boron-containing transition metal clusters and metallaboranes, and, more recently on carborane derivatives. She has written two books: 'Boranes and Metallaboranes: Structure, Bonding and Reactivity' (Ellis Horwood) and 'Clusters of the *p*-Block Elements' (OUP).



related to their borane parents.<sup>7</sup> Here, the isolobal analogy is important – if the frontier molecular orbitals of two fragments possess the same symmetry characteristics, are of roughly the same energy, and contain the same number of electrons, the fragments are isolobal. Thus, {BH} is isolobal with  $\{Ru(CO)_3\}$  (as well as with a wide variety of other fragments) (Figure 1) and a BH unit can, in theory, be exchanged for an  $\{Ru(CO)_3\}$  fragment. Of course there are also steric constraints to be taken into account, and distortion of the parent borane cage is to be expected as a more sterically demanding metal unit is introduced in place of a boron-based unit. This is illustrated in Figure 2 by the structures of the  $B_{5-}M_{-}$ -cores of  $B_5H_9$ ,  $[Fe_2(CO)_6B_3H_7]$ ,<sup>8</sup>  $[Cp^*Co_2B_3H_7]$ ,<sup>9</sup> and  $[Ru_3(CO)_8(PPh_3)B_2H_6]$ ,<sup>10</sup> all are *nido*-clusters, related by the isolobal analogy  $(BH \equiv Fe(CO)_3 \equiv Ru(CO)_3 \equiv Ru(CO)_2(PPh_3) \equiv Cp^*Co)$ . By electron counting rules, each is described as possessing a square-based pyramidal geometry.

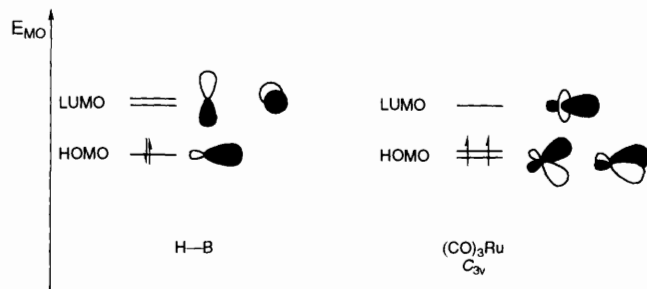


Figure 1 The frontier orbitals of the {BH} and  $C_{3v}$   $\{Ru(CO)_3\}$  units illustrating that the two fragments are interchangeable in clusters as far as their bonding capabilities are concerned.

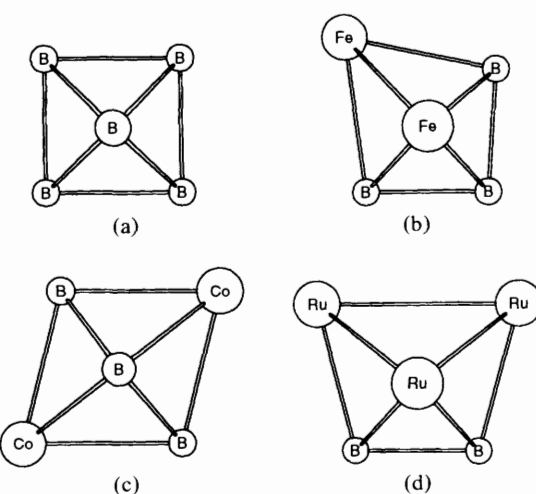


Figure 2 The square-based pyramidal cores (viewed from above) of the *nido*-clusters (a)  $B_5H_9$ , (b)  $[Fe_2(CO)_6B_3H_7]$ , (c)  $[Cp^*Co_2B_3H_7]$ , and (d)  $[Ru_3(CO)_8(PPh_3)B_2H_6]$ .

Abbreviations. v.e., valence electrons; EAN, effective atomic number; PSEPT, polyhedral skeletal electron pair theory; Cp,  $\eta^5$ -cyclopentadienyl; Cp\*,  $\eta^5$ -pentamethylpentadienyl.

Beginning with a particular borane, we can use the isolobal analogy to introduce successive metal fragments. Hence, we progress from a borane to a boron-rich metallaborane (defined here as a cluster in which boron still dominates over metal), on to a metal-rich metallaborane (still with the boron and metal atoms in the vertex positions of the cage), and then to an all-metal cluster. Note that this is only a *formal* progression – it is not usual in an experimental setting simply to take a borane and replace the boron units one by one by metal-centred fragments. Nonetheless many compounds are known that are isolobal analogues of one another, even if their synthetic origins are independent.

Once the metal cage is formed, there is the potential for a new kind of boron environment – the interstitial site within a metal cage may be able to accommodate a boron atom, and the discrete metal boride cluster is born. Solid-state metal borides are well documented,<sup>11</sup> and of significant interest is the fact that the structural motifs that are present in the bulk solid sometimes replicate those found in the discrete compounds. Moreover, Fehlner and his group have shown that molecular transition-metal boride clusters such as  $[\text{HFe}_4(\text{CO})_{12}\text{BH}_2]$  can be used as precursors to thin-film materials with the retention of the metal boron ratio.<sup>11b</sup>

This review is concerned largely with metal-rich metallaboranes and with methods of encouraging B–H bonds to transform into B–M interactions, thereby converting a metallaborane into a metallaboride cluster, or at least starting the transformation sequence. The methods employed do not begin with a deltahedral borane cage – the largest borane precursor that we have used is  $[\text{B}_3\text{H}_8]^-$ , and indeed Lewis base adducts of  $\text{BH}_3$  have proved to be invaluable precursors in this work. Although the synthetic strategy is generally not one of isolobal fragment replacement, application of the isolobal principle is an important method of choosing reagents and planning reaction sequences.

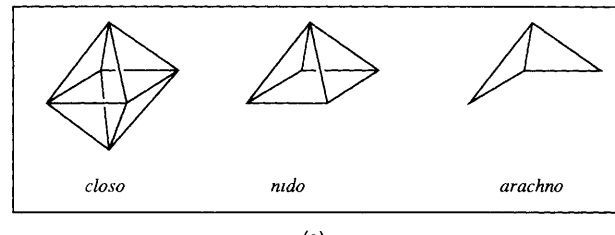
In keeping with the aims of *Chemical Society Reviews*, this article is not intended to be a comprehensive survey of the area, and, where appropriate, reference is made to several reviews of the area<sup>12–17</sup> in preference to the primary literature.

## 2 Structure Types and Electron Counting

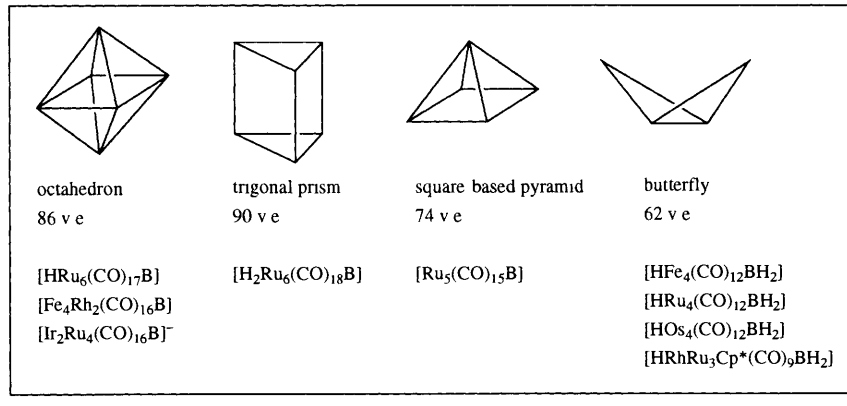
The bonding in transition metal clusters is generally approached either by use of PSEPT or the effective atomic number (EAN) rule.<sup>18</sup> Figure 3(a) shows the relationship between the *closo*-octahedron, *nido*-square-based pyramid, and *arachno*-butterfly geometries, by PSEPT, all require 7 pairs of cluster bonding electrons. Figure 3(b) shows the number of valence electrons associated with each of these metal-atom cage structures within the EAN approach. The common ‘parent’ geometries within PSEPT are deltahedra ( $\Delta$ -faces) with between 5 and 12 vertices. Thus, the trigonal prism [Figure 3(b)] would be classified as a *hypho*-cluster. This geometry is not favoured by members of the borane family, but *does* feature quite regularly in low oxidation state metal cluster chemistry. There are other features observed in metal cage structures that are uncommon in boron chemistry (*e.g.* capped faces, bridged edges, and spikes) and which are, perhaps, more readily dealt with within the framework of the EAN method of electron counting than within PSEPT. No doubt some readers will argue over this point, but for the purposes of this review, we shall restrict the discussion to the use of the EAN rule.

The term *boride* is used to indicate that a boron atom is interstitially sited within a metal cavity – similarly, carbide, nitride, and phosphide clusters feature interstitial carbon, nitrogen, or phosphorus atoms. When in this environment, the boron atom contributes all three of its valence electrons to cluster bonding. Thus the 90 v.e. count which is consistent with a trigonal prismatic geometry is obtained for the boride cluster  $[\text{H}_2\text{Ru}_6(\text{CO})_{18}\text{B}]^-$  as follows:

$$\begin{aligned}
 2 \text{ H} &= 2 \text{ v.e.} \\
 6 \text{ Ru} &= 6 \times 8 = 48 \text{ v.e.} \\
 18 \text{ CO} &= 18 \times 2 = 36 \text{ v.e.} \\
 \text{B} &= 3 \text{ v.e.} \\
 1 - \text{charge} &= 1 \text{ v.e.} \\
 \hline
 & 90 \text{ v.e.}
 \end{aligned}$$

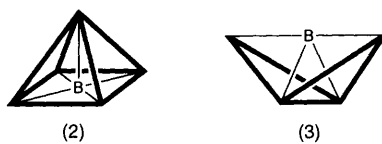


(a)



(b)

**Figure 3** (a) The octahedral, square-based pyramidal and butterfly geometries all require the same number of cluster bonding electrons within PSEPT. (b) Examples of electron counting by the EAN rule. Note that it is common to refer to the two different sites in the 62 v.e. butterfly framework as ‘hinge’ and ‘wingtip’.



Boron atoms, like some other *p*-block elements,<sup>19</sup> are not always fully encapsulated within a metal cage. Structures (2) and (3) show two possible environments, and the term 'semi-interstitial', is appropriate to these situations, in particular to structure (3) where the boron atom is very exposed. When the boron atom is in a semi-interstitial site, an ambiguity in electron counting may occur. The first 'test-case' came with  $[\text{HFe}_4(\text{CO})_{12}\text{BH}_2]$ <sup>20</sup> (Figure 4) which retains two B–H interactions, although these are bridging rather than terminal. Interestingly this cluster historically predates the fully interstitial borides. Consideration was given to both the electronic structure of  $[\text{HFe}_4(\text{CO})_{12}\text{BH}_2]$ , and to the geometrical parameters of the tetra-iron framework (in particular, the internal dihedral angle of the butterfly), and the conclusion was that the boron atom behaves *not* as a vertex but as an interstitial atom. Note that the boron atom lies only 0.3 Å above the  $\text{Fe}_{\text{wingtip}}\text{---Fe}_{\text{wingtip}}$  axis. Thus, despite being involved in B–H bonding interactions, all three of the valence electrons of the boron are used in cluster bonding. The electron count is then as follows

$$\begin{aligned}
 3 \text{ H} &= 3 \text{ v e} \\
 4 \text{ Fe} &= 4 \times 8 = 32 \text{ v e} \\
 12 \text{ CO} &= 12 \times 2 = 24 \text{ v e} \\
 \text{B} &= 3 \text{ v e} \\
 \hline
 62 \text{ v e}
 \end{aligned}$$

which is consistent with a butterfly framework of four (metal) atoms. Note that the boron atom is *not* a framework atom, but is buried within the framework.

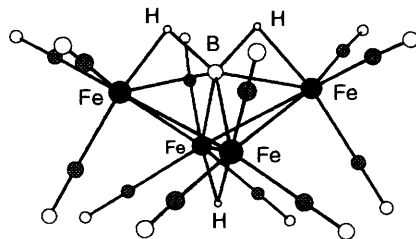


Figure 4 The structure of  $[\text{HFe}_4(\text{CO})_{12}\text{BH}_2]$

### 3 The Role of $^{11}\text{B}$ NMR Spectroscopy

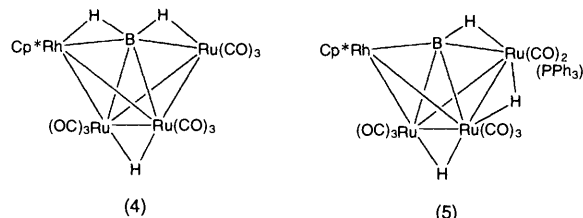
As boride cluster chemistry has developed,  $^{11}\text{B}$  NMR spectroscopy has played an important role in the prediction of approximate cluster type. Of course, the diversity of structure in these molecular systems means that the results of *X*-ray crystallography are the only sure way of defining details of cluster geometry. However Rath and Fehlner<sup>21</sup> have developed a parameterized model for ferraborane clusters, permitting new  $\delta^{11}\text{B}$  shifts to be fitted to possible structural types. The method partitions a chemical shift value into contributions due to direct Fe–B, bridging Fe–H–B, terminal B–H, *etc* interactions. In our own work, we have found that a similar model can be used with remarkable success within the area of ruthenium–boron chemistry. The key lies in the fact that the  $^{11}\text{B}$  chemical shift range is relatively large, and the values of  $\delta^{11}\text{B}$  are extremely sensitive to the environment of the boron atom.

The  $^{11}\text{B}$  NMR chemical shifts may be correlated with boron Mulliken populations (calculated at the Fenske–Hall level), and the large shielding caused by Fe–B interactions has been related

to an increase in the multiple bond contributions to the shielding tensor. The sign and magnitude of the paramagnetic contribution to the shielding correlates well with experimental  $^{11}\text{B}$  spectral shift data.<sup>21,22</sup>

### 4 Ligand Exchange and Competitive Boron-abstraction

The substitution of a carbonyl ligand in a cluster for another two-electron donor ligand may alter the electron distribution in the cage with the result that the location of the cluster-bond hydrogen atoms changes. In some cases, this reorganization can be a step towards denuding the boron atom of B–H interactions, thus increasing the boron-to-metal bonding. An example is seen when the 62 v.e. butterfly-cluster  $[\text{HRhRu}_3(\text{Cp}^*)(\text{CO})_9\text{BH}_2]$  (4) reacts with  $\text{PPh}_3$ . The phosphine ligand substitutes for one of the ruthenium-bound carbonyl ligands, and there is an associated migration of an Rh–H–B bridging hydrogen atom into an Ru–H–Ru site such that this hydrogen atom attaches itself to the same ruthenium atom as the phosphine ligand. The product is  $[\text{H}_2\text{RhRu}_3(\text{Cp}^*)(\text{CO})_9\text{BH}]$  (5).<sup>23</sup>



Although this particular migration strips one hydrogen atom from the boron centre, one related migration actually *increases* the number of B–H interactions. During the reaction of  $[\text{HFe}_4(\text{CO})_{12}\text{BH}_2]$  (see Section 5) with  $\text{PMe}_2\text{Ph}$ , substitution occurs at a wingtip site as in (4), but this time a Fe–H–Fe (hinge) hydrogen atom migrates to an Fe–H–B site – *i.e.* migration towards the phosphine this time coincides with migration towards the boron atom.<sup>13</sup>

Reactions of boron centres with Lewis bases, in particular in small boranes, can result in cleavage of the borane and adduct formation. In the clusters  $[\text{M}_3(\text{CO})_9\text{BH}_5]$  and  $[\text{M}_3(\text{CO})_9\text{BH}_4]$  ( $\text{M} = \text{Fe}$  or  $\text{Ru}$ ), either a borohydride-like or  $\text{BH}_3$ -like unit is present. In  $[\text{HRu}_3(\text{CO})_9\text{B}_2\text{H}_5]$ , a  $\{\text{B}_2\text{H}_5\}$ -moiety is bound to the triruthenium framework. The behaviour of some of these clusters towards Lewis bases has been investigated with interesting results. The ferraborane anion  $[\text{Fe}_3(\text{CO})_9\text{BH}_4]$  is degraded by  $\text{PMe}_2\text{Ph}$  via two competitive pathways which illustrate that the Lewis base will attack both the boron and iron centres.<sup>12,13</sup> Similarly, both boron and metal centres in  $[\text{HRu}_3(\text{CO})_9\text{B}_2\text{H}_5]$  react with  $\text{PPh}_3$ .<sup>10</sup> One pathway gives  $[\text{HRu}_3(\text{CO})_8(\text{PPh}_3)\text{B}_2\text{H}_5]$  and  $[\text{HRu}_3(\text{CO})_7(\text{PPh}_3)_2\text{B}_2\text{H}_5]$  with retention of the  $\text{Ru}_3\text{B}_2$ -core, and this competes with boron-abstraction (as the adduct  $\text{Ph}_3\text{P}^+\text{BH}_3$ ) to give the clusters  $[\text{Ru}_3(\text{CO})_{9-x}(\text{PPh}_3)_x\text{BH}_5]$  ( $x = 1–3$ ). The relevance of this reaction to the theme of the article is as follows.

The ruthenaborane  $[\text{Ru}_3(\text{CO})_9\text{BH}_5]$  exists as a mixture of isomers (Figure 5a) which differ only in the position of one hydrogen atom. In solution, these isomers are equally favoured. In the family  $[\text{Ru}_3(\text{CO})_{9-x}(\text{PPh}_3)_x\text{BH}_5]$  ( $x = 1–3$ ), each phosphine ligand is attached to a different ruthenium atom. The introduction of the  $\text{PPh}_3$  groups into the metal triangle causes the isomer equilibrium shown in Figure 5a to shift to the right-hand side. In the solid-state structure of  $[\text{Ru}_3(\text{CO})_6(\text{PPh}_3)_3\text{BH}_5]$  [Figure 5(b)], the hydrogen atoms have been located crystallographically and the result is consistent with solution data ( $^{11}\text{B}$ ,  $^{31}\text{P}$ , and  $^1\text{H}$  NMR spectroscopies). A greater degree of direct B–Ru bonding is present in the phosphine derivative than in the nonacarbonyl parent compound.

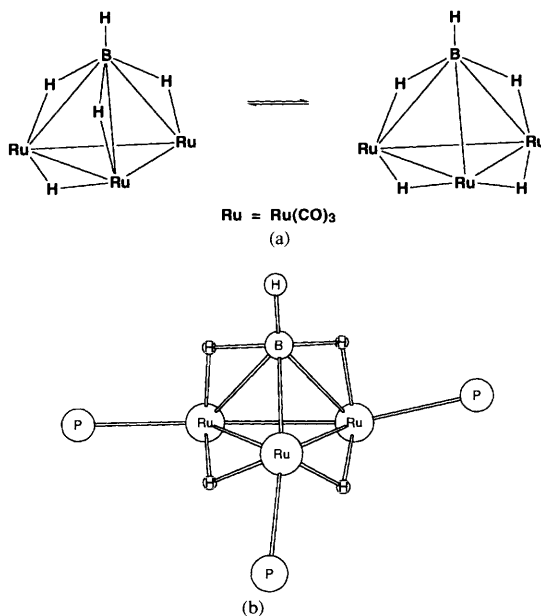
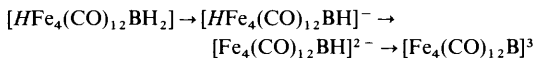


Figure 5 (a) The two isomers of  $[\text{Ru}_3(\text{CO})_9\text{BH}_5]$ , (b) the structure of the core of  $[\text{Ru}_3(\text{CO})_6(\text{PPh}_3)_3\text{BH}_5]$  confirmed by  $X$ -ray crystallography

## 5 Deprotonation

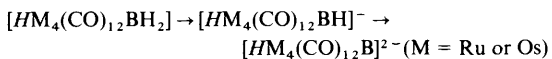
The deprotonation of many of the metal-rich metallaboranes so far investigated occurs *via* the loss of a boron-bound proton with a concomitant increase in the degree of direct metal–boron bonding. One exception is  $[\text{HRu}_3(\text{CO})_9\text{B}_2\text{H}_5]$  which loses  $\text{H}^+$  from an Ru–H–Ru site.

Mostly, only monoanions have been formed and studied, but successive deprotonations of the butterfly compounds  $[\text{HM}_4(\text{CO})_{12}\text{BH}_2]$  ( $\text{M} = \text{Fe, Ru, Os}$ ) have been achieved.<sup>13,16,17</sup> The pattern of deprotonations is metal-dependent. The structures of each of the three compounds are related (Figure 4). Work from Fehlner's group shows that loss of protons from  $[\text{HFe}_4(\text{CO})_{12}\text{BH}_2]$  follows the sequence



where the italicised  $\text{H}$  is metal-only bound, and the remaining  $\text{H}$  atoms are in Fe–H–B bridging positions (see Figure 4). The tri-anion is a rare example of a truly semi-interstitial boron atom, as illustrated schematically in structure (3).

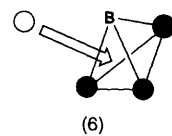
Shore and co-workers have studied the successive loss of *two* protons from  $[\text{HRu}_4(\text{CO})_{12}\text{BH}_2]$  and  $[\text{HOs}_4(\text{CO})_{12}\text{BH}_2]$



and the formation of  $[\text{HRu}_4(\text{CO})_{12}\text{BH}]^-$  has been studied independently in our group. For  $\text{M} = \text{Ru or Os}$ , the boron-bound hydrogen atoms are both lost in preference to the M–H–M bridge, leading to the formation of a cluster with a core with structure (3).

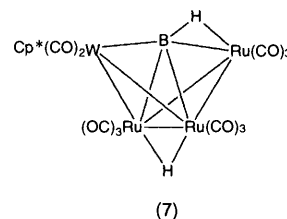
## 6 Changing the Heterometal Fragment

On paper at least, we can propose a series of clusters in the butterfly family that have one or more of the group 8  $\text{M}(\text{CO})_3$  metal fragments replaced by other fragments. In this way heterometallic systems with varying electronic structures can be envisaged. Synthetically, we can make use of the fact that clusters with the  $\text{M}_3\text{B}$ -core may undergo expansion with the addition of a metal fragment to one of the triangular  $\text{M}_2\text{B}$ -faces, as shown schematically in structure (6).<sup>12–14,17</sup> This method



was first used in Fehlner's group to give a quantitative conversion from  $[\text{Fe}_3(\text{CO})_9\text{BH}_4]^-$  to  $[\text{HFe}_4(\text{CO})_{12}\text{BH}]^-$  and its application to the synthesis of heterometallic species has proved successful, for example in the reaction of  $[\text{Ru}_3(\text{CO})_9\text{BH}_4]^-$  with  $\{\text{Cp}^*\text{RhCl}_2\}_2$  to give cluster (4), and in the photolysis of  $[\text{Ru}_3(\text{CO})_9\text{BH}_5]$  with  $[\text{Fe}(\text{CO})_5]$  to give  $[\text{HFeRu}_3(\text{CO})_{12}\text{BH}_2]$ .

This building-block approach does indeed denude the boron atom of some of its B–H interactions, but we can take the strategy one step further by choosing metal fragments that provide *more* electrons to the cluster. In this way we can reduce the need for the number of cluster hydrogen atoms. (The butterfly cluster consistently requires 62 v.e.) An example is the reaction of  $[\text{Ru}_3(\text{CO})_9\text{BH}_5]$  with  $\{\text{CpW}(\text{CO})_3\}_2$  which leads to  $[\text{HRu}_3\text{W}(\text{Cp})(\text{CO})_{11}\text{BH}]$  (7). The  $\{\text{CpW}(\text{CO})_2\}$ -unit provides one more electron for cluster bonding than does, say, a  $\{\text{Cp}^*\text{Rh}\}$ -unit. Thus in comparing structures (4) and (7), we observe that the cage responds to the difference by 'losing' a cluster-hydrogen atom.



However, reaction pathways are not always as expected. We saw above that treatment of  $[\text{Ru}_3(\text{CO})_9\text{BH}_4]^-$  with  $\{\text{Cp}^*\text{RhCl}_2\}_2$  leads to the 62 v.e. cluster (4), but if  $\{\text{Cp}^*\text{IrCl}_2\}_2$  replaces its rhodium analogue, the product is the 64 v.e. cluster  $[\text{H}(\text{Cp}^*\text{Ir})\text{Ru}_3(\text{CO})_{10}\text{BH}_2]$  (Figure 6(a)), the structure can be described as an 'open-butterfly'. The iridium centre carries an extra CO ligand which cannot readily be removed in order to force the cluster to 'collapse' down to the 62 v.e. butterfly framework. Attempts to introduce a  $\{\text{Cp}^*\text{Ru}\}$ -fragment to the cluster have lead to an unusual 'spiked-butterfly' species  $[\text{H}_2\text{Ru}_5(\text{Cp}^*)(\text{CO})_{13}\text{BH}_2]$  (Figure 6(b)) instead of the anticipated 62 v.e. butterfly  $[\text{H}_2\text{Ru}_4(\text{Cp}^*)(\text{CO})_9\text{BH}_2]$ . Sometimes a greater than expected degree of boron encapsulation results and an exciting example from our work has been the reaction of  $[\text{Ru}_3(\text{CO})_9\text{BH}_4]^-$  with  $\{\text{Rh}(\text{CO})_2\text{Cl}\}_2$  which leads both to the octahedral boride  $[\text{Rh}_2\text{Ru}_4(\text{CO})_{16}\text{B}]^-$  and the capped double-trigonal prismatic diboride  $[\text{Rh}_3\text{Ru}_6(\text{CO})_{23}\text{B}_2]$  which is described in Section 7.

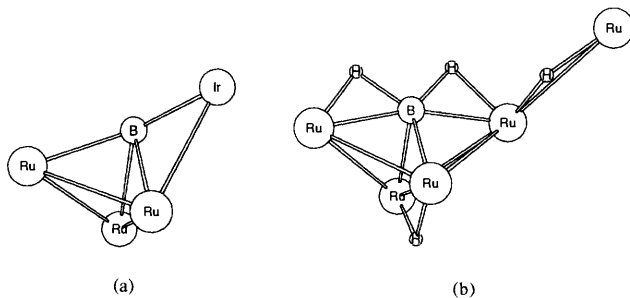
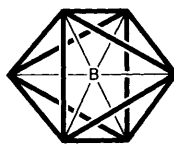


Figure 6 The metal–boron core structures of (a)  $[\text{H}(\text{Cp}^*\text{Ir})\text{Ru}_3(\text{CO})_{10}\text{BH}_2]$  and (b)  $[\text{H}_2\text{Ru}_5(\text{Cp}^*)(\text{CO})_{13}\text{BH}_2]$ . Hydrogen atoms were located and are shown in (a), but were not located in (b). Spectroscopic data are consistent with the presence of one Ru–H–Ru and two Ru–H–B bridges. Two isomers are present in solution.

## 7 Building-up Metal Cages ( $n > 4$ )

To date, most high-nuclearity metal  $M_n$ -cages ( $n > 4$ ) comprise group 8 metals, although Fehlner has also reported results involving cobalt. This section describes some of the systematic approaches, and also provides some insight into the more intriguing cluster shapes that can be formed.

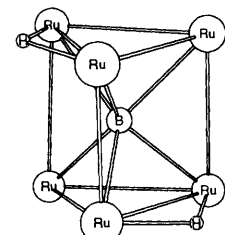


(8)

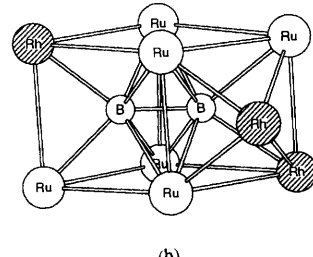
As in the previous section, a ‘building-block’ approach has proved to be an invaluable route.<sup>13 14 17</sup> A comparison of structures (3) and (8) illustrates that the addition of two vertices (two metal fragments) to a butterfly cluster containing a semi-interstitial boron atom should yield a closed octahedral boride. In this state, the boron atom is completely denuded of hydrogen atoms. The first true boride cluster was prepared by Fehlner and co-workers by the reaction of  $[\text{HFe}_4(\text{CO})_{12}\text{BH}]^-$  (or other derived anions) with  $[\{\text{Rh}(\text{CO})_2\text{Cl}\}_2]$ . The thermodynamically stable product is *trans*- $[\text{Fe}_4\text{Rh}_2(\text{CO})_{16}\text{B}]^-$  but through  $^{11}\text{B}$  NMR spectral monitoring, it was possible to observe the initial formation of the *cis*-isomer. The *cis*  $\rightarrow$  *trans* isomerization, including the kinetics of the process, has been studied in detail. Rather surprisingly, attempts to obtain the conjugate acid of  $[\text{Fe}_4\text{Rh}_2(\text{CO})_{16}\text{B}]^-$  by protonation yielded *mer*- $[\text{H}_2\text{Fe}_3\text{Rh}_3(\text{CO})_{15}\text{B}]$ . In our group we have investigated the reactions of  $[\text{HRu}_4(\text{CO})_{12}\text{BH}]^-$  with  $[\{\text{Rh}(\text{CO})_2\text{Cl}\}_2]$ , and with  $[\{\text{IrL}_2\text{Cl}\}_2]$  [ $\text{L}_2$  = (cyclooctene)<sub>2</sub> or cod] and CO. We observe a preference for the *trans*-isomers of both the octahedral borides  $[\text{Rh}_2\text{Ru}_4(\text{CO})_{16}\text{B}]^-$  and  $[\text{Ir}_2\text{Ru}_4(\text{CO})_{16}\text{B}]^-$ , although for the rhodium-containing cluster, minor amounts of the *cis*-isomer are also observed in solution. The addition of  $[\text{AuP}(\text{C}_6\text{H}_{11})_3]^+$  (introduced as the chloride) leads to a mixture of both *cis*- and *trans*-isomers of  $[\text{Rh}_2\text{Ru}_4(\text{CO})_{16}\text{B}\{\text{AuP}(\text{C}_6\text{H}_{11})_3\}]$  but only *cis*- $[\text{Ir}_2\text{Ru}_4(\text{CO})_{16}\text{B}\{\text{AuP}(\text{C}_6\text{H}_{11})_3\}]$ . The cluster *cis*- $[\text{Rh}_2\text{Ru}_4(\text{CO})_{16}\text{B}\{\text{AuP}(\text{C}_6\text{H}_{11})_3\}]$  rapidly isomerizes to *trans*- $[\text{Rh}_2\text{Ru}_4(\text{CO})_{16}\text{B}\{\text{AuP}(\text{C}_6\text{H}_{11})_3\}]$ . A parallel set of reactions can be carried out using  $[\text{Ph}_3\text{PAuCl}]$ . The gold(I) fragment remains on the periphery of the central hexametal cage. The ability of the  $\text{M}_2\text{Ru}_4$ -cage ( $\text{M}$  = Rh or Ir) metal cage to undergo isomerization processes of this type is consistent with the stabilizing effect that an interstitial atom has on the metal array that surrounds it.<sup>24</sup>

The first fully characterized homometallic  $\text{M}_6\text{B}$ -boride,  $[\text{HRu}_6(\text{CO})_{17}\text{B}]$ ,<sup>13 17</sup> was reported by Shore, and was prepared by the reaction of  $[\text{Ru}_3(\text{CO})_{12}]$  with  $\text{BH}_3$  in THF at 75 °C. Independently we had developed a route to the conjugate base of  $[\text{HRu}_6(\text{CO})_{17}\text{B}]$  by treating  $[\text{Ru}_3(\text{CO})_{12-x}(\text{NCMe})_x]$  ( $x = 1$  or 2) with  $\text{BH}_3$  in the presence of  $\text{NMe}_3$ , but we also found that the triruthenaborane  $[\text{Ru}_3(\text{CO})_9\text{BH}_5]$  [Figure 5(a)] undergoes a light-induced cluster-assembly reaction to give  $[\text{HRu}_4(\text{CO})_{12}\text{BH}_2]$  and  $[\text{HRu}_6(\text{CO})_{17}\text{B}]$ . Single crystal data for  $[\text{HRu}_6(\text{CO})_{17}\text{B}]$  confirmed the presence of a fully interstitial boron atom in an octahedral  $\text{Ru}_6$ -cage, but two isomers (differing primarily in the arrangement of the CO ligands) have been structurally characterized. Each isomer has a different synthetic origin.

Although the assembly of  $[\text{HRu}_6(\text{CO})_{17}\text{B}]$  from  $[\text{Ru}_3(\text{CO})_9\text{BH}_5]$  is a convenient synthesis of this boride cluster, we argued that a logical route would be to ‘sandwich’ together the  $\{\text{Ru}_3\}$ - and  $\{\text{Ru}_3\text{B}\}$ -units by reacting  $[\text{Ru}_3(\text{CO})_{12-x}(\text{NCMe})_x]$  ( $x = 1$  or 2) with  $[\text{Ru}_3(\text{CO})_9\text{BH}_5]$  or its conjugate base. In fact, a far better, but related, synthetic route is to combine  $[\text{Ru}_3(\text{CO})_{12-x}(\text{NCMe})_x]$  with  $[\text{Ru}_3(\text{CO})_9\text{B}_2\text{H}_5]^-$ , and this leads not only to the 86 v.e. octahedral  $[\text{Ru}_6(\text{CO})_{17}\text{B}]^-$  but also to the 90 v.e. trigonal prismatic anion  $[\text{H}_2\text{Ru}_6(\text{CO})_{18}\text{B}]^-$ .



(a)

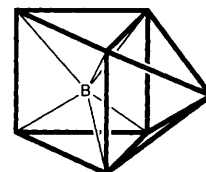


(b)

Figure 7 The core structures of (a) the trigonal prismatic  $[\text{H}_2\text{Ru}_6(\text{CO})_{18}\text{B}]^-$ , and the capped double trigonal prismatic  $[\text{Rh}_3\text{Ru}_6(\text{CO})_{23}\text{B}_2]^-$

[Figure 7(a)] The octahedral and prismatic cages are, of course, related in having two  $\text{Ru}_3$ -triangles either mutually staggered or eclipsed, and the formal interconversion is accompanied by a four-electron oxidation or reduction. To date, however, we have not been able to bring about this transformation in a controlled manner, (but see Section 8) It seems more likely that in the synthesis, the two hexaruthenium cluster anions are formed by independent pathways rather than *via* one another.

The anion  $[\text{H}_2\text{Ru}_6(\text{CO})_{18}\text{B}]^-$  was the first *molecular* example of a boron atom interstitially sited in a trigonal prismatic cavity, although this structural unit is present in the binary ruthenium boride  $\text{Ru}_7\text{B}_3$ .<sup>11</sup> Further developments lead to the synthesis (see Section 6) of the capped double-trigonal prismatic diboride  $[\text{Rh}_3\text{Ru}_6(\text{CO})_{23}\text{B}_2]^-$  [Figure 7(b)] and once again we observed that boron sited in both octahedral and trigonal prismatic cavities could be generated in a single reaction – a second product from the reaction of  $[\text{Ru}_3(\text{CO})_9\text{BH}_4]^-$  with  $[\{\text{Rh}(\text{CO})_2\text{Cl}\}_2]$  was the 86 v.e. anion  $[\text{Rh}_2\text{Ru}_4(\text{CO})_{16}\text{B}]^-$ , previously prepared as described earlier in this section. Note though that it would seem that neither of these borides is formed in a systematic fashion, although the  $\{\text{Ru}_3\text{B}\}$ -core present in the precursor  $[\text{Ru}_3(\text{CO})_9\text{BH}_4]^-$  is a structural motif in the product  $[\text{Rh}_3\text{Ru}_6(\text{CO})_{23}\text{B}_2]^-$  [Figure 7(b)].



(9)

Fehlner’s group has recently<sup>25</sup> observed a similar trigonal prismatic cavity but in a heptanuclear species, namely  $[\text{HFe}_7(\text{CO})_{20}\text{B}]^{2-}$  (9). This is one of the products from the reactions between  $[\text{Fe}_4(\text{CO})_{12}\text{BH}]^{2-}$  and  $[\text{Fe}_2(\text{CO})_9]$  or  $[\text{Fe}(\text{CO})_3(\text{cyclooctene})]$ . Two other iron borides which are formed are  $[\text{HFe}_6(\text{CO})_{17}\text{B}]^{2-}$  (for which a *nido*-geometry has been proposed) and  $[\text{HFe}_5(\text{CO})_{15}\text{B}]^{2-}$ . This latter dianion is related to  $[\text{HOs}_5(\text{CO})_{16}\text{B}]$  [Figure 8(a)] prepared and crystallographically characterized by Shore and co-workers.<sup>16</sup> This was the first example of a fully interstitial boron atom in an osmium cage.

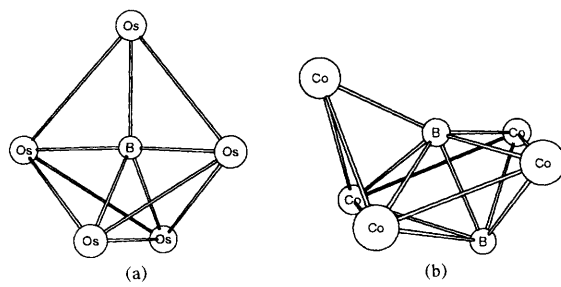


Figure 8 The metal–boron core structures of (a)  $[\text{HOs}_5(\text{CO})_{16}\text{B}]$  and (b)  $[\text{Co}_5(\text{CO})_{14}\text{B}(\text{BH})]$

Shore has pioneered the chemistry of osmium–boron (metal-rich cluster) chemistry and has successfully denuded the boron atom of its hydrogen atoms even in a cluster of low nuclearity. Hydroboration of  $[\text{H}_2\text{Os}_3(\text{CO})_{10}]$  leads to  $[\text{H}_3\text{Os}_3(\text{CO})_9\text{B}(\text{CO})]$ , the wide-ranging chemistry of which<sup>15 16 26</sup> includes its use as a precursor to  $[\text{HOs}_5(\text{CO})_{16}\text{B}]$  and  $[\text{HOs}_4(\text{CO})_{12}\text{BH}_2]$ .

Cobalt boride chemistry is not so well advanced as the group 8 work, but as long ago as 1975, Schmid *et al.* reported  $[\text{Co}_6(\text{CO})_{18}\text{B}]$ , formed from  $[\text{Co}_2(\text{CO})_8]$  and  $\text{BBr}_3$  or diborane(6)<sup>27</sup> However, it must be noted that the odd-electron count for this proposed cluster (93 e<sup>-</sup>) fits neither the octahedron nor the trigonal prism (Figure 3). A fully characterized cobalt boride of formula  $[\text{Co}_5(\text{CO})_{14}\text{B}(\text{BH})]$  has been prepared in Fehlner's group from the reaction of  $[\text{Co}_2(\text{CO})_8]$  and  $\text{BH}_3\text{SMe}_2$  (75 °C). The core structure [Figure 8(b)] is most unusual and has only one of the boron atoms in a boridic environment (within bonding contact with all five cobalt atoms)<sup>17</sup>

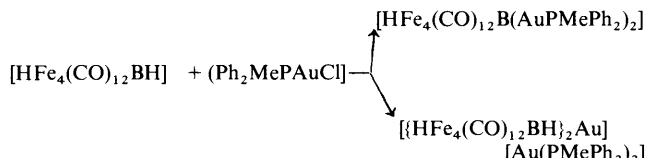
## 8 Reactions with Group 11 Electrophiles

Over the past eight years or so, our group has been especially interested with the reactions of boron-containing cluster anions with group 11 electrophiles, and in particular gold(i) phosphines.<sup>13 17</sup> It is well established that these metal fragments tend to bind to the periphery of a metal cluster rather than become an integral part of a perceivable metal polyhedral skeleton.<sup>28</sup> However, when in a semi-interstitial site as shown in structure (3), the boron atom may become a centre around which gold(i) units aggregate. Initial results were obtained from the reaction of  $[\text{HFe}_4(\text{CO})_{12}\text{BH}]^-$  with  $[\text{Ph}_3\text{PAuCl}]$  which gave  $[\text{Fe}_4(\text{CO})_{12}\text{BH}(\text{AuPPh}_3)_2]$  in which the boron retained a B–H interaction but added two B–Au bonding interactions. However, by reducing the steric requirements of the phosphine ligand, hydrogen-migration can be encouraged and we wit-

nessed an isomer equilibrium between the forms  $[\text{Fe}_4(\text{CO})_{12}\text{BH}(\text{AuPR}_3)_2]$  and  $[\text{HFe}_4(\text{CO})_{12}\text{B}(\text{AuPR}_3)_2]$ , where 'BH' indicates an Fe–H–B bridging hydrogen atom and the italicized *H* is metal-only bound. The core structure of  $[\text{HFe}_4(\text{CO})_{12}\text{B}(\text{AuPEt}_3)_2]$  (the minor isomer in this case) is shown in Figure 9(a), the cluster hydrogen atom bridges the hinge Fe–Fe edge [the lowest edge in Figure 9(a)] but was not located in the crystal structural analysis. This  $\text{Fe}_4\text{BAu}_2$ -core structure predominates for phosphine ligands with relatively small Tolman cone angles, whilst for sterically demanding phosphines (for example a combined Tolman cone angle for the two phosphines  $\geq 290^\circ$ ), none of this isomer is observed, and the boron atom retains a B–H interaction.

The introduction of three gold(i) units can readily be achieved by using the oxonium salt  $[(\text{AuPPh}_3)_3\text{O}]^+[\text{BF}_4]^-$  and reaction with  $[\text{HFe}_4(\text{CO})_{12}\text{BH}]^-$  leads to  $[\text{Fe}_4(\text{CO})_{12}\text{B}(\text{AuPPh}_3)_3]$  [Figure 9(b)] in which the three gold atoms are all attached to the boron atom giving the latter a connectivity of seven (4 Fe + 3 Au). A similar 7-coordinate environment for the boron atom is observed in  $[\{\text{HRu}_4(\text{CO})_{12}\text{B}\}_2\text{Cu}_4(\mu\text{-Cl})]$  which is described in Section 9. Recently, Schmidbaur has used the  $[(\text{AuPPh}_3)_3\text{O}]^+$  cation to generate the novel boron-centred cation  $[(c\text{-C}_6\text{H}_{11})_3\text{PB}(\text{AuPPh}_3)_4]^+$  in which the boron atom is at the apex of a square-based pyramidal arrangement of one boron and four gold atoms.<sup>29</sup>

We have also observed that competition may arise between the pathway leading to the products of addition of the gold(i) phosphine fragments, and one in which a Au–P bond is cleaved and cluster fusion takes place. This was first noted in the reaction of  $[\text{HFe}_4(\text{CO})_{12}\text{BH}]^-$  with  $[\text{Ph}_2\text{MePAuCl}]$



The route to the fused species was found to be particularly favoured when the metal butterfly framework comprised ruthenium rather than iron atoms and the cluster anion  $[\{\text{HRu}_4(\text{CO})_{12}\text{BH}\}_2\text{Au}]^-$  [Figure 9(c)] has been fully characterized as the  $[(\text{Ph}_3\text{P})_2\text{N}]^+$  salt. The gold centre is formally in a +1 oxidation state, and hence the coordination environment about this centre is usefully described as being 'pseudo-linear'. This follows from a description of each B–Au–Ru interaction being considered a three-centre two-electron one.

An analogous fusion of butterfly units occurs when  $[(\text{Ph}_3\text{P})_2\text{N}][\text{HRu}_4(\text{CO})_{12}\text{BH}]$  reacts with  $[\text{Ag}(\text{NCMe})_4]^+$ , and the product is  $[(\text{Ph}_3\text{P})_2\text{N}][\{\text{HRu}_4(\text{CO})_{12}\text{BH}\}_2\text{Ag}]$ . However,

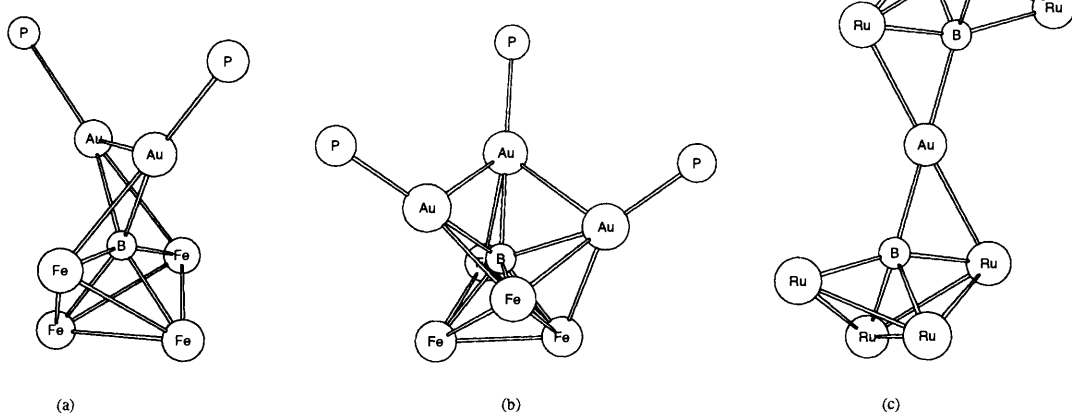


Figure 9 Metal–boron core structures of (a)  $[\text{HFe}_4(\text{CO})_{12}\text{B}(\text{AuPEt}_3)_2]$  (b)  $[\text{Fe}_4(\text{CO})_{12}\text{B}(\text{AuPPh}_3)_3]$ , and (c)  $[\{\text{HRu}_4(\text{CO})_{12}\text{BH}\}_2\text{Au}]$

when the metal electrophile is  $[\text{Cu}(\text{NCMe})_4]^+$ , a more intriguing cluster-assembly is observed. The bright red product has been confirmed by *X*-ray crystallography to be  $\{[\text{HRu}_4(\text{CO})_{12}\text{BH}_2]_2\text{Cu}_4(\mu\text{-Cl})\}$  (Figure 10), and its silver analogue is a second product of the reaction of  $[\text{Ag}(\text{NCMe})_4][\text{BF}_4]$  with  $[(\text{Ph}_3\text{P})_2\text{N}][\text{HRu}_4(\text{CO})_{12}\text{BH}]$ . The source of the chloride ligand is thought to be  $[(\text{Ph}_3\text{P})_2\text{N}]\text{Cl}$ . The compound  $\{[\text{HRu}_4(\text{CO})_{12}\text{BH}_2]_2\text{Cu}_4(\mu\text{-Cl})\}$  co-crystallizes with  $[(\text{Ph}_3\text{P})_2\text{N}]\text{Cl}$  and we have been unable to remove this salt. In  $\{[\text{HRu}_4(\text{CO})_{12}\text{BH}_2]_2\text{Cu}_4(\mu\text{-Cl})\}$ , two  $\{\text{HRu}_4(\text{CO})_{12}\text{BH}_2\}$ -sub-clusters are fused through a tetrahedral  $\{\text{Cu}_4\}$ -subcluster, one edge of which is bridged by a chloride ligand. Each boron atom is involved in bonding interactions to four ruthenium and three copper atoms, and the 7-coordinate geometry is similar to that observed in  $[\text{Fe}_4(\text{CO})_{12}\text{B}(\text{AuPPPh}_3)_3]$  (Figure 9(b)). A feature of particular interest is the ambiguity in copper oxidation state. Each ruthenaborane sub-cluster is formally a dianion, leaving an overall +4 charge associated with the  $\{\text{Cu}_4(\mu\text{-Cl})\}$ -unit. However, there is no evidence that the species is paramagnetic.

The trigonal prismatic anion  $[\text{H}_2\text{Ru}_6(\text{CO})_{18}\text{B}]^-$  (Figure 7(a)) reacts with  $[\text{Ph}_3\text{PAuCl}]$  and  $[(2\text{-MeC}_6\text{H}_4)_3\text{PAuCl}]$  with concomitant rearrangement of the hexaruthenium cage around the interstitial atom – each of the resultant mono-, di-, and tri-gold

derivatives possesses an octahedral  $\text{Ru}_6\text{B}$ -core. As above, the tri-gold derivative is best accessed using gold(i) oxonium salts. As yet, we have been unable to prepare derivatives  $[\text{Ru}_6(\text{CO})_{17}\text{B}]^-$  which retain the prismatic core. The conversions from trigonal prismatic into octahedral  $\text{Ru}_6\text{B}$ -core have been confirmed by the results of crystal structure determinations of  $[\text{Ru}_6(\text{CO})_{17}\text{B}\{\text{AuP}(2\text{-MeC}_6\text{H}_4)_3\}]$ ,  $[\text{HRu}_6(\text{CO})_{16}\text{B}\{\text{AuPPPh}_3\}_2]$ , and  $[\text{Ru}_6(\text{CO})_{16}\text{B}\{\text{AuPPPh}_3\}_3]$  (Figure 11). The octahedral anion  $[\text{Ru}_6(\text{CO})_{17}\text{B}]^-$  may also be used as a precursor for these ‘gold-plated’ clusters. (Related systems were described in Section 7.) The mono-gold derivative  $[\text{Ru}_6(\text{CO})_{17}\text{B}(\text{AuPPPh}_3)]$  has found application as a precursor to a pentaruthenium boride. Under a pressure of CO, a ruthenium carbonyl vertex is extruded from  $[\text{Ru}_6(\text{CO})_{17}\text{B}(\text{AuPPPh}_3)]$  to give  $[\text{Ru}_5(\text{CO})_{15}\text{B}(\text{AuPPPh}_3)]$  (Figure 11(d)). Note how, in comparison to its location in the precursor (Figure 11(a)), the boron atom has moved out of and below the plane of the four ruthenium atoms that now define the basal plane in the square-based pyramidal  $\text{Ru}_5$ -core of  $[\text{Ru}_5(\text{CO})_{15}\text{B}(\text{AuPPPh}_3)]$ . In addition, the gold(i) phosphine unit has swung down to become intimately associated with the boron atom as well as the original two ruthenium centres.

## 9 Cluster Fusion

In Section 8, examples of fusing  $\text{Ru}_4\text{B}$ -butterfly units through mono- or tetrametal units of the group 11 triad were described. During these cluster-fusion reactions which began with the conjugate base of  $[\text{HRu}_4(\text{CO})_{12}\text{BH}_2]$ , the boron atom gained either one or three B–M interactions at the expense of one or two B–H interactions with respect to its environment in  $[\text{HRu}_4(\text{CO})_{12}\text{BH}_2]$ .

Fehlner has reported<sup>30</sup> a sequence of reactions that takes the diserraborane  $[\text{Fe}_2(\text{CO})_6\text{B}_2\text{H}_6]$  to the fused system  $\{[\text{Fe}_2(\text{CO})_6\text{B}_2\text{H}_4\}_2$  (Figure 12). During the sequence, the boron is denuded of B–H bonds whilst increasing its degree of boron–iron and/or boron–boron bonding. The salt  $\text{Li}_2[\text{Fe}_2(\text{CO})_6\text{B}_2\text{H}_4]$  is formed by the deprotonation of  $[\text{Fe}_2(\text{CO})_6\text{B}_2\text{H}_6]$  using  $\text{Bu}^n\text{Li}$ .

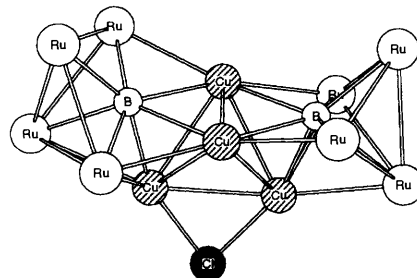


Figure 10 The structure of the cluster-core of  $\{[\text{HRu}_4(\text{CO})_{12}\text{BH}_2]_2\text{Cu}_4(\mu\text{-Cl})\}$ , in the compound  $\{[\text{HRu}_4(\text{CO})_{12}\text{BH}_2]_2\text{Cu}_4(\mu\text{-Cl})\}[(\text{Ph}_3\text{P})_2\text{N}]\text{Cl}$

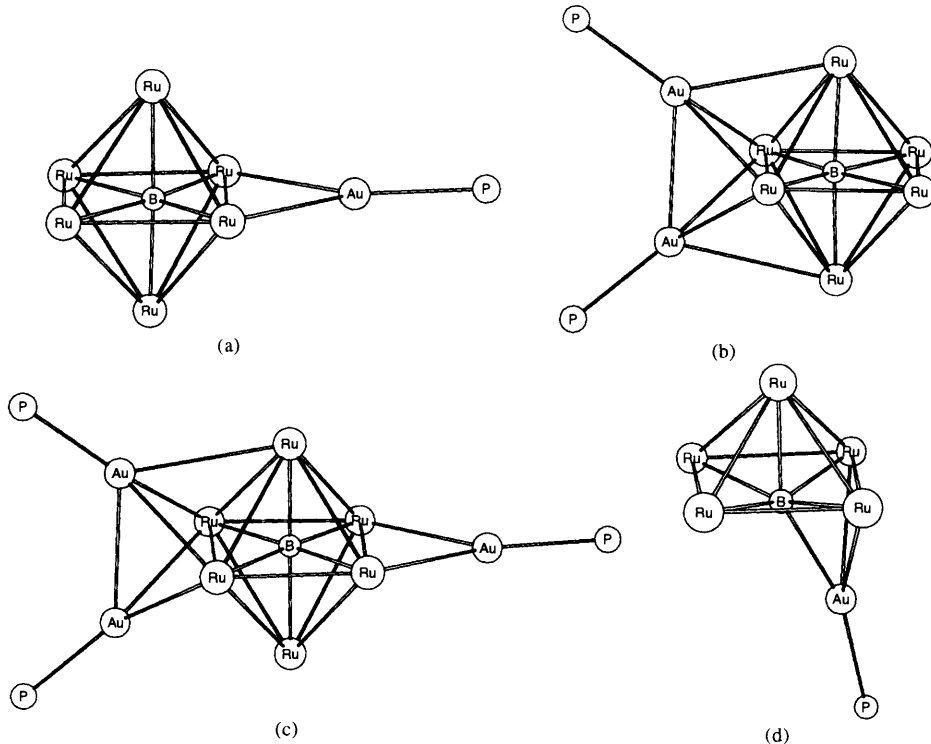
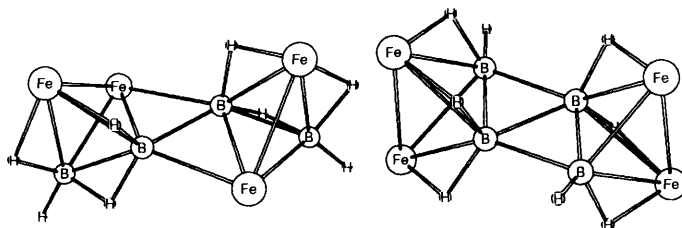


Figure 11 The core structures of (a)  $[\text{Ru}_6(\text{CO})_{17}\text{B}\{\text{AuP}(2\text{-MeC}_6\text{H}_4)_3\}]$ , (b)  $[\text{HRu}_6(\text{CO})_{16}\text{B}(\text{AuPPPh}_3)_2]$ , (c)  $[\text{Ru}_6(\text{CO})_{16}\text{B}(\text{AuPPPh}_3)_3]$ , and (d)  $[\text{Ru}_5(\text{CO})_{15}\text{B}(\text{AuPPPh}_3)]$  (carbonyl, hydride, and aryl groups are omitted)



**Figure 12** The structures of the cores of the *B Fe-conjuncto* and *B B-conjuncto* isomers of  $[\{Fe_2(CO)_6B_2H_4\}_2]$

(controlled conditions) Oxidative fusion of the dianion gives  $[B,Fe\text{-conjuncto}-\{Fe_2(CO)_6B_2H_4\}_2]$ , and thermolysis of this compound leads to the *B,B-conjuncto*-isomer which exhibits three tautomers in solution

## 10 Conclusions

In this article we have seen a variety of methods by which boron atoms in metallaborane clusters can be denuded of one or more B–H interactions. The outcome of these transformations has been the formation both of metallaborane clusters which possess a greater degree of direct metal-to-boron interaction, and a series of metallaboride clusters, some of which place the boron atom in 6- and 7-coordinate environments. In such a site, the boron atom is quite unlike that in a borane (or carbaborane) cluster, and is more similar to that found in solid-state metal borides. Further, an interstitial boron atom can assist in the stabilization of a metal framework and facilitate isomerization processes which involve the metal cage.

**Acknowledgements** My own contributions to this area have been made possible by the excellent contributions from past and present members of my research group (postdoctoral, graduate students, and undergraduate project students whose names appear in the references) and by the crystallographic expertise of Arnie Rheingold (University of Delaware). Acknowledgement is given to the Donors of the Petroleum Research Fund administered by the American Chemical Society for financial support, to the Royal Society, and to the SERC for studentships.

## 11 References

- 1 N N Greenwood and A Earnshaw, 'Chemistry of the Elements', Pergamon Press, Oxford, 1984
- 2 C E Housecroft, Boranes and Metallaboranes Structure, Bonding and Reactivity, 2nd Edn, Ellis Horwood, Hemel Hempstead, 1994

- 3 C E Housecroft, Cluster Molecules of the *p*-Block Elements, Oxford University Press, Oxford, 1994
- 4 K Wade, *Adv Inorg Chem Radiochem*, 1976, **18**, 1
- 5 R E Williams, *Adv Inorg Chem Radiochem*, 1976, **18**, 67
- 6 D M P Mingos, *Nature*, 1972, **236**, 99
- 7 J D Kennedy, *Prog Inorg Chem*, 1984, **32**, 519, *ibid*, 1986, **34**, 211
- 8 K J Haller, E L Andersen, and T P Fehlner, *Inorg Chem*, 1981, **20**, 309
- 9 Y Nishihara, K J Deck, M Shang, and T P Fehlner, *J Am Chem Soc*, 1993, **115**, 12224
- 10 C E Housecroft, D M Matthews, A J Edwards, and A L Rheingold, *J Chem Soc Dalton Trans*, 1993, 2727
- 11 See for example (a) N N Greenwood, R V Parish, and P Thornton, *Quart Rev Chem Soc*, 1966, **20**, 441, (b) T P Fehlner, *Adv Inorg Chem*, 1990, **35**, 199 and references therein
- 12 T P Fehlner, *New J Chem*, 1988, **12**, 307 and references therein
- 13 C E Housecroft, *Adv Organomet Chem*, 1991, **33**, 1 and references therein
- 14 T P Fehlner in Electron Deficient Boron and Carbon Clusters, ed G A Olah, K Wade, and R E Williams, Wiley, New York, 1991, ch 12, p 287 and references therein
- 15 D P Workman and S G Shore, in Electron Deficient Boron and Carbon Clusters, ed G A Olah, K Wade, and R E Williams, Wiley, New York, 1991, ch 10, p 237 and references therein
- 16 S G Shore, *Pure Appl Chem*, 1994, **66**, 263 and references therein
- 17 C E Housecroft, *Coord Chem Rev*, 1995, (in press), and references therein
- 18 D M P Mingos and D J Wales, 'Introduction to Cluster Chemistry', Prentice Hall, Englewood Cliffs, 1990, and references therein
- 19 C E Housecroft, in 'Inorganometallic Chemistry' (Modern Inorganic Chemistry Series), ed T P Fehlner, Plenum, New York, 1992, ch 3, p 73
- 20 T P Fehlner, C E Housecroft, W R Scheidt, and K S Wong, *Organometallics*, 1983, **2**, 825
- 21 N P Rath and T P Fehlner, *J Am Chem Soc*, 1988, **110**, 5345
- 22 R Khattar, T P Fehlner, and P T Czech, *New J Chem*, 1991, **15**, 705, T P Fehlner, P T Czech, and R F Fenske, *Inorg Chem*, 1990, **29**, 3103
- 23 J R Galsworthy, C E Housecroft, D M Matthews, R Ostrander, and A L Rheingold, *J Chem Soc Dalton Trans*, 1994, 69
- 24 J R Galsworthy, A D Hattersley, C E Housecroft, A L Rheingold, and A Waller, *J Chem Soc Dalton Trans*, 1995, 549
- 25 A Bandyopadhyay, M Shang, C S Jun, and T P Fehlner, *Inorg Chem*, 1994, **33**, 3677
- 26 D-Y Jan, D P Workman, L-Y Hsu, J A Krause, and S G Shore, *Inorg Chem*, 1992, **31**, 5123 and references therein
- 27 G Schmid, V Batzel, G Etzrodt, and R Pfeil, *J Organomet Chem*, 1975, **86**, 257
- 28 I D Salter, *Adv Organomet Chem*, 1989, **29**, 249 and references therein
- 29 A Blumenthal, H Beruda, and H Schmidbaur, *J Chem Soc Chem Commun*, 1993, 1005
- 30 C-S Jun, D R Powell, K J Haller, and T P Fehlner, *Inorg Chem*, 1993, **32**, 5071